Latest Advances In Ion Implantation & Annealing For Gate And Channel (USJ) Doping Optimization

John Borland[1], Wade Krull[2], Masayasu Tanjyo[3], Mark Namaroff[4], and Andrzej Buczkowski[5]
[1]J.O.B. Technologies, 98-1204 Kuawa St. Aiea, Hawaii 96701, USA
[2]SemEquip, 34 Sullivan Rd., N. Billercia, MA 01862, USA
[3]Nissin Ion Equipment, 575, Kuze-Tonoshiro-Cho, Minami-Ku, Kyoto, 601-8205, Japan
[4]Axcelis Technologies, 108 Cherry Hill Dr., Beverly, MA 01915, USA
[5]Nanometrics, 1320 SE Armour Dr., Suite B-2, Bend, OR 97702, USA
E-mail : JohnOBorland@aol.com

1. Introduction

The number of implant steps are increasing with each device generation, for example with SOC (system on a chip) devices this can average around 38 implant steps for low and high voltage transistors. Implant micro and macro dopant precision and variation directly affects device Vt variability as reported by Yoneda and Niwayama [1] and also by Kuroi and Kawasaki [2] for high current (HC) implantation. Therefore, detection and monitoring of any variation in the precision of implanted dopant is critical to reduce device Vt variation as devices are scaled to the 45nm and 32nm nodes.

2. High Current

High current implanters are the largest implant market segment averaging >51% of the total implant market for the last 3 years and greatest implant strategic added value to device processing. Over the next 2 years HC implanter designs must change to address 2 distinct device requirements:

1) The DRAM dual poly gate (DPG) structure requires a compensating very high dose boron implant in the 1E16 to 1E17/cm^2 dose range. The process choices are $B_{18}H_{22}$ molecular implant in the 1-3E16/cm^2 dose range on traditional beam-line HC implanters or plasma implantation in the 1-2E17/cm^2 dose range using BF_3 or B_2H_6 source materials.

2) The 32nm node USJ doping requirement of 50-100eV equivalent energy for boron while maintaining a retained dose of 1E15/cm^2. The 50-100eV equivalent energies can be realized by using molecular dopant species like $B_{18}H_{22}$ for p-type dopant and P_4 or As_4 for n-type dopant using SemEquip ClusterIon source on traditional HC implanters.

Compensating p+ dual poly gate doping

For a 60nm thick poly gate, a 3.5keV B equivalent energy is desired, as reported by Parrill and Rubin [3]. With plasma doping, the dopants are piled-up at the surface and decline exponentially in depth. Beam-line implantation produces the classic Gaussian-like profile where the majority the dopant is deeper and retrograde at the surface. Comparative examples of these profiles have been shown by Qin and McTeer [4], and are reproduced in Fig.1a as-implanted and Fig.1b&c post anneal. Decel-mode beam-line implantation can not be used because any boron energy contamination will penetrate through the gate and add dopant to the channel region. Plasma doping has additional issues, such as BF_3 plasma etching the silicon while B_2H_6 plasma leads to surface deposition. However, both plasma doping and beam-line implantation with $B_{18}H_{22}$ are being used for DPG manufacturing starting at the 70nm DRAM node as press released by both Varian [5] and Axcelis [6].

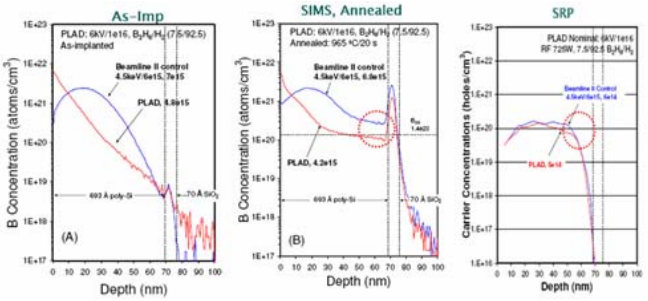

Fig. 1 : Plasma versus beam-line boron implantation dopant profiles : a) as implanted before annealing SIMS dopant profile, b) after anneal SIMS dopant profile and c) SRP dopant profile [4].

Ultra Shallow Junction

The Xj target for the 45nm node is 12-20nm, requiring B energy to be 200-500eV. However, for 32nm node the targeted Xj is between 8-15nm after anneal. This drives the B implant energy down to between 50-100eV, which would produce an as implanted Xj=5-6nm if a pre-amorphizing implant (PAI) is used to prevent boron dopant channeling as shown in Fig. 2. In this range, conventional HC tools must use decel-mode, which leads to energy contamination. The shallow junction requirement places tight constraints on allowable energy contamination, usually <0.1%, constraining decel tools to low decel ratios, typically <3 to 1. The BF_2 option would require energy in the range of 250-500eV, but residual implant damage, end of range (EOR) defects and other adverse effects of fluorine make this option less desirable, as reported by Borland, et al. [7]. Using $B_{18}H_{22}$, the operational energy would be 1-2keV in drift mode and avoiding the defect issues with BF_2 and PAI+B implants. Another issue for junctions below 10nm is the retained boron dose after implant and annealing, as shown in Fig. 3 [8]. The Bss (boron solid solubility) activation data shown in Fig. 3 is for Flash annealing at >1300^{o}C where an activation level of 1E20/cm^3 is realized until the retained dose drops below 6E14/cm^2. With a retained dose of 3E14/cm^2 an activation level of only 5E19/cm^3 is realized for BF_2 therefore, at low energies, retained dose and total activation levels varies with each implant technology. Since enhanced B dopant activation

was reported when using $B_{18}H_{22}$ with advanced annealing techniques such as Flash, laser and SPE retained dose may not be a major concern as it is with BF_2 (see Fig. 4) [7].

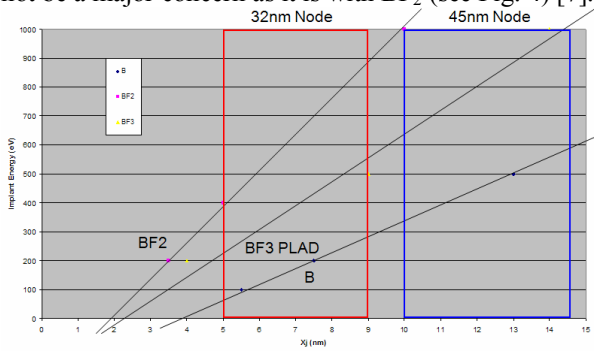

Fig. 2 : Boron implant energy versus depth.

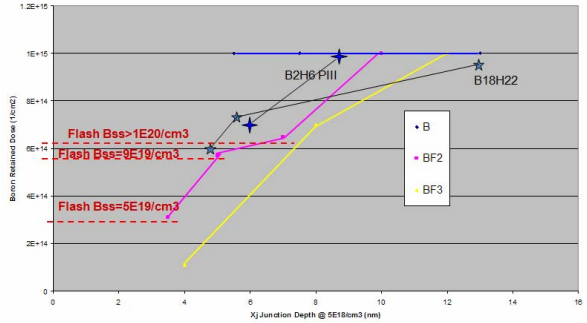

Fig. 3 : Retained boron dose for various B dopant species.

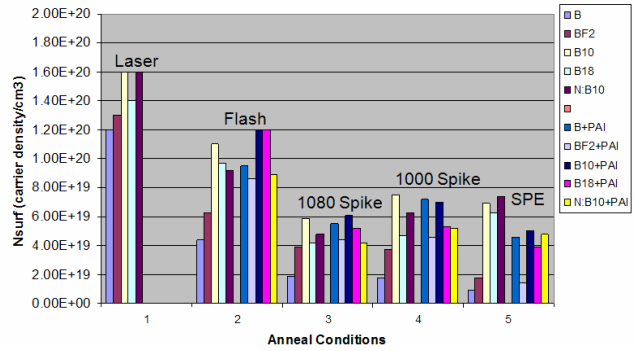

Fig. 4 : Enhanced dopant activation with $B_{18}H_{22}$.

Serial HC implanter design

Single wafer HC implanter replaced batch type due to gate poly yield failure as first reported by Kawasaki [9]. Each HC implant vendor has a different serial wafer end-station design including scanning mechanism resulting in a unique non-uniformity signature caused by local and global variation in implant precision due to dose and angle control. Any variation in localized implant angle will result in asymmetrical transistor, Vt & gate length variation and gate delay degradation as reported by Kuroi [2]. Detecting these localized implant micro-variation with HC implantation requires 0.05-0.1mm pitch metrology tool resolution. Figs. 5 & 6 shows thermawave diameter line scan results with a 5mm versus 1mm pitch measurement resolution comparing 3 different serial HC implanters. Note that a left to right variation signature pattern can be detected on the ribbon beam implanter with either the 5mm or 1mm measurement pitch in Fig. 5 while top to bottom line scans showing a 2mm variation in localized implant uniformity for the ribbon beam and a 6mm variation in localized implant uniformity for the spot beam 2D mechanical scan HC implanters required the 1mm measurement pitch and could not be detected with the 5mm pitch and as shown in Fig. 6. For more detail, a 0.1mm or even a 50um pitch measurement for detecting these micro-variation is required. Sheet resistance (Rs) measurements by 4PP with a 1mm pitch resolution is also shown in Figs. 5 & 6 showing good correlation to the TW micro-variation results. Surface photo voltage (SPV) wafer maps and diameter scans for a spot beam with 2-D mechanical scan is shown in Fig. 7 and after anneal in Fig. 8 [10]. Note the unique local micro-variation signature showing a peak to valley local variation of 11.5% and peak spacing of 42mm. After anneal the lamp annealer bulls-eye pattern can be detected. Fig. 9 shows the SPV signature map of the ribbon beam implanter with 18% global variation.

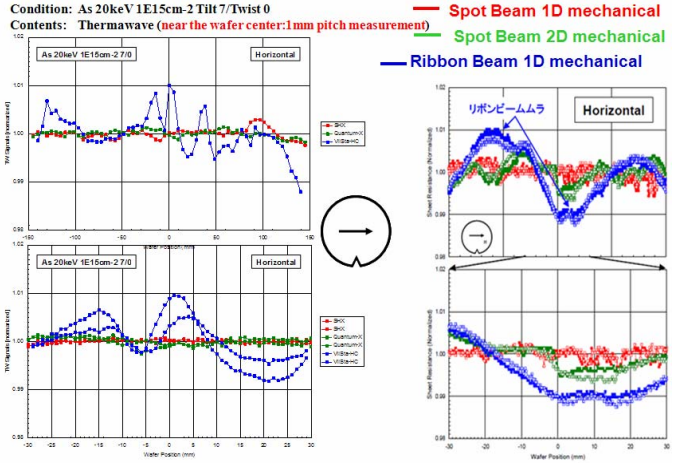

Fig. 5 : Left to right TW and 4PP local variation.

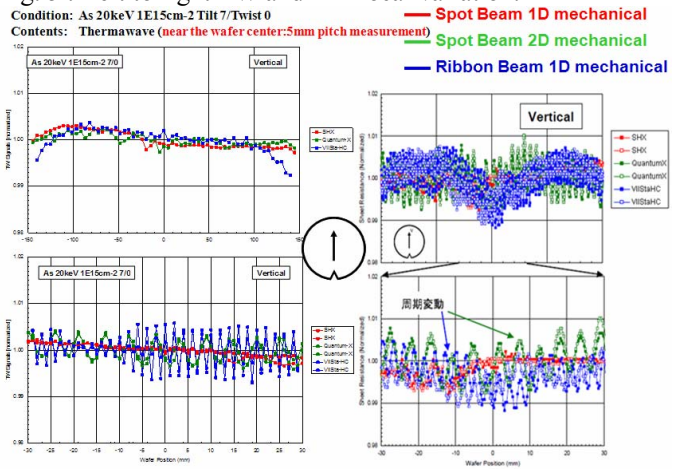

Fig. 6 : Top to bottom TW and 4PP local variation.

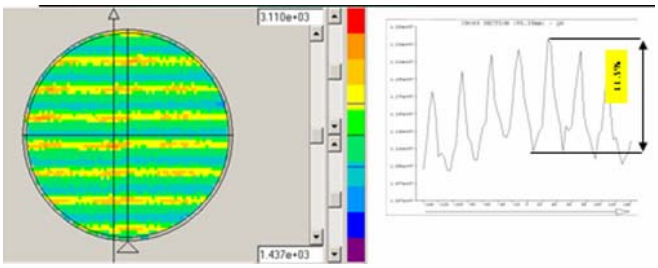

Fig. 7 : SPV wafer map of spot beam with 2-D scanning [10].

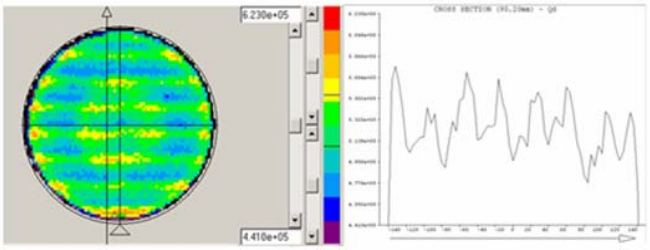

Fig. 8: SPV wafer map after annealing [10].

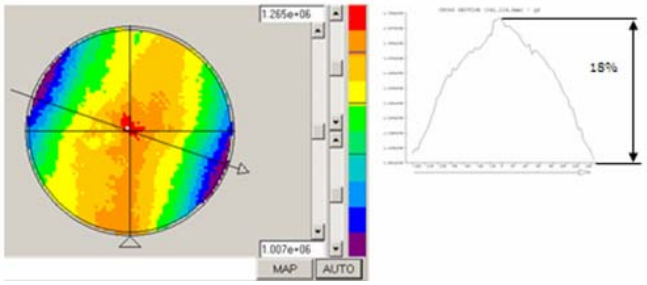

Fig. 9: SPV wafer map of ribbon beam [10].

The ribbon beam global variation can be reduced but not eliminated by going to quad-mode and even tilted implantation as reported by Erokin [11]. Adding quad-mode implantation changes the global variation signature from a paint brush like striping left to right to a 4 fold symmetry pattern as shown below in Fig. 10 using therma-wave analysis. For spot beam with 2D mechanical scan uniformity can be improved by changing the beam spot size and number of scans (scan pitch).

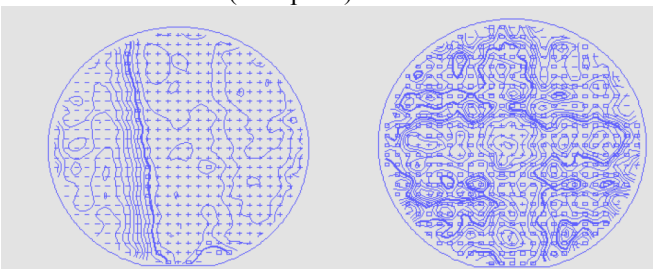

Fig. 10: TW wafer map of ribbon beam with single versus quad-mode scanning.

When the electrical dopant activation level (Bss) is 10x to 100x below the chemical level then dose variation is not critical and this is especially true for boron. With arsenic this difference is only about 2-5x. Also, with soak or spike RTA annealing with >15nm of dopant diffusion, the as-implanted non-uniformity is usually washed out but with diffusion-less activation the as-implanted signature becomes the final after anneal signature, so detection and monitoring of these effects is important. It is also important to know the diffusion-less activation annealer signature which can also contribute to both global and micro-localized device variation as shown in Figs. 11 & 12 for Flash and laser annealed wafers characterized by photoluminence (PLi).

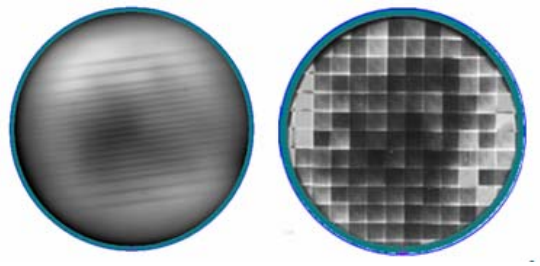

Fig. 11: PLi maps of: a) Flash and b) laser annealed wafers.

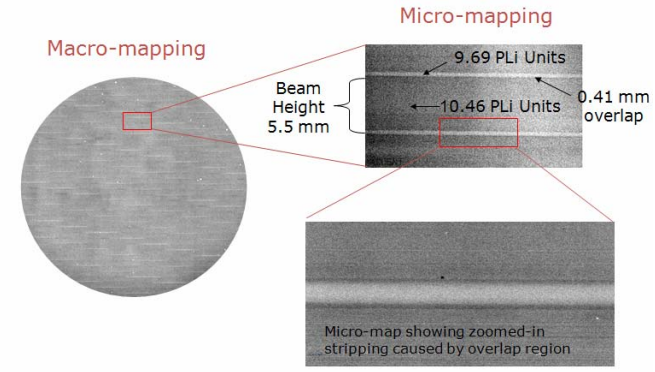

Fig. 12: PLi laser annealed wafer map in a) macro and b) micro mode.

Besides the different unique serial implant signatures discussed above and shown in Figs. 5-10, msec Flash and laser annealing equipment also has their unique annealing non-uniformity signatures. PLi wafer image shows the signature of each Xe-lamp in Fig. 11a and the EM-4PP Rs diameter line scan measurement is shown in Fig. 13. The localized variation in arsenic dopant activation (Rs sheet resistance) caused by the lamp signature can be about 23%. Improvements are being made by design changes for uniform thermal heating across the wafer in combination with lower temperature spike annealing and this can reduce wafer global variation by 4x and local micro-variation by 3x.

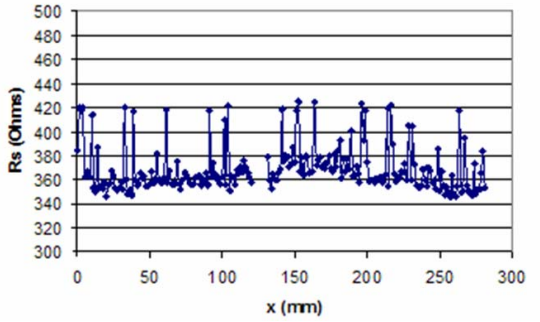

Fig. 13: EM-4PP showing local Rs variation from Flash annealing.

3. Medium Current

Medium current implanters make up about 31% of the total implant market and the implant equipment vendors are pushing both the high energy limits and low energy limits. Over the last few years the upper energy limit for charge state 3 (X+++) has increased from 750keV to 900keV for retrograde n-well implants as specified on the VIISta-900XP from Varian and Exceed-9600AH from Nissin while the lower energy limit went from 5keV to

500eV to meet the lower energy requirements for HALO and pocket implants as specified on the Optima-MD from Axcelis.

At the lower energies below 5keV beam blow-up can be an issue as reported by Aoyama [12] showing 150mm spot beam size for B at 5keVwhile switching to $B_{10}H_{14}$ reduced the beam spot size to only 10mm. Similar improvements can also be realized with $B_{18}H_{22}$. At high tilt angles the on wafer beam spot size could change significantly resulting in huge variation of dopant precision (angle and dose) across a 300mm device wafer due to the implantation shadowing effects caused by the gate stack structure during the HALO or pocket high tilt implant resulting in top to bottom across wafer device variation as reported by Suguro of Toshiba [13] and illustrated below in Fig.14.

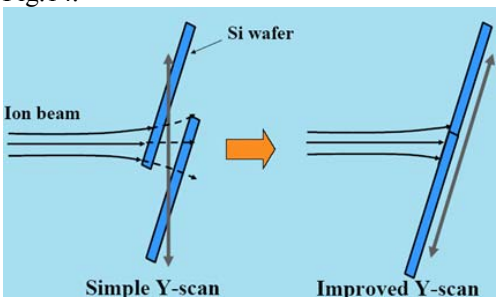

Fig. 14: Boron HALO iso-scanning effects [13].

Using iso-centric scanning to maintain constant focal length is one solution available on the Optima-MD from Axcelis and Exceed-Nx from Nissin medium current implanters. Another option is to use higher mass dopant species such as molecular dopant species ($B_{10}H_{14}$, $B_{18}H_{22}$, As_4, and P_4) or In & Sb which would require higher energy implants avoiding beam blow-up. However, In and Sb dopants may lead to residual implant damage and EOR defects that degrades junction quality/leakage with msec annealing. As the industry moves to diffusion-less annealing starting at the 45nm node, multiple HALO implants will be used for precise SCE (short channel effect) and gate length control requiring extreme implant precision with minimal variation as reported by Narihiro of NEC [14]. Similarly, multiple tilted extension implantations are being studied for SCE optimization with diffusion-less activation and this also leads to lateral graded single source drain structures as reported by Borland et al [15].

4.Summary

High current implanters are now all single wafer but they all have a unique, correctable, dopant micro-variation signature that can only be detected and monitored with <0.1mm pitch spatial resolution. The various advanced millisecond annealing equipment also have their unique micro and macro annealing variation signatures that can either add to or hide the implant dopant variations so new metrology techniques with <0.1mm step resolution is needed. Medium current implanters have extended their upper energy range to 900keV and lower energy range to 500eV. For high tilt implantation such as the multiple HALO implant, precision will require constant focal length and therefore iso-centric scanning motion and higher mass dopant species implants to achieve retrograde and dopant free channels with diffusion-less annealing techniques.

Acknowledgements

The authors are grateful to Pierre Mitchell of Therma-Wave for some of the TW results and to Robert Hillard of Solid State Measurements for the EM-4PP localized Rs results.

References

[1] K. Yoneda and M. Niwayama, "The Drain Current Asymmetry of 130nm MOSFETs Due to Extension Implant Shadowing Originated by Mechanical Angle Error in High Current Implantation," IWJT, 2002, Section S2-3, p. 19.

[2] T. Kuroi and Y. Kawasaki, "Ultra-shallow Junction Formation for 45nm node and beyond," USJ, 2005, p. 4.

[3] T. Parrill and L. Rubin, "Transistor Scaling is Moving Implant Energies Lower ," *Solid State Technology*, June 2005, p. 61.

[4] S. Qin and A. McTeer, "Device Performance Evaluation of PMOS Devices Fabricated by B2H6 PIII/PLAD Process on Poly-Si Gate Doping," IWJT, 2006, p. 68.

[5] "Industry-Leading Memory Manufacturer Selects VIISta PLAD for High-Dose Dual Poly Gate Implant ," Varian Semiconductor Equipment Associates Inc. Press Release, July 25, 2006.

[6] "Axcelis Announces Key Design Win at Major Asian Memory Chipmaker for New Optima HD Imax Molecular Implant System," Axcelis Technologies Inc. Press Release, Oct. 3, 2006.

[7] J. Borland et al., "High Dopant Activation and Low Damage p+ USJ Formation," IIT, June 2006.

[8] J. Borland, "Process Variability Reduction For Gate Doping and USJs ," *Semiconductor International*, December 2006, Vol. 29, No. 13, p. 49.

[9] Y. Kawasaki et al., "The Collapse of Gate Electrode in High Current Implantation of Batch Type," IWJT, 2004, p. 39.

[10] C. Krueger et al., "Surface Charge Profiling: An Advancement in Ion Implant Monitoring", IIT-2006, to be published.

[11] Y. Eurokin and J. Liu, "Precision Implant Requirements for SDE Junction Formation in Sub-65nm CMOS Devices," IWJT, 2006, p. 21.

[12] T. Aoyama et al., "Decaborane Ion Implantation for sub-40nm Gate Length PMOS-FETs to Enable Formation of Steep Ultra-shallow Junction and Small Threshold Voltage Fluctuation," IWJT, 2005, Section S2-2, p. 27.

[13] K. Suguro, "Prospects and Challenges in USJ Technologies For Next Generation LSIs," vTech presentation, July 2005.

[14] M. Narihiro et al., "Sub-30nm MOSFET Fabrication Technology Incorporating Precise Dopant Profile Design Using Diffusion-less High Activation Laser Annealing," IEEE RTP, October 2006, p. 147.

[15] J. Borland et al., "High-Tilt Implant and Diffusion-less Activation for Lateral Graded S/D Engineering ," *Solid State Technology*, June 2003, p. 52.